Journal of Electronic Materials (2024) 53:298–311
https://doi.org/10.1007/s11664-023-10770-7

ORIGINAL RESEARCH ARTICLE

Planetary Ball Milling and Tailoring of the Optoelectronic Properties of Monophase SnSe Nanoparticles

A. G. Kunjomana[1] · J. Bibin[1,2,3] · R. C. Athira[1] · M. Teena[4]

Received: 11 May 2023 / Accepted: 4 October 2023 / Published online: 31 October 2023

Abstract

Downscaling of tin monoselenide (SnSe) samples to the nanometer regime (~80–20 nm) without affecting the structure, homogeneity, and optoelectronic properties was carried out by high-energy planetary ball milling (BM). The milling rate was varied from 200 rpm to 800 rpm by adopting a dry and wet-grinding top-down approach on customized stoichiometric SnSe precursors. The degree of crystallinity was assessed by powder x-ray diffraction (PXRD) and selected area electron diffraction. The lattice parameters, $a = 4.435$ Å, $b = 11.498$ Å, and $c = 4.148$ Å, of the nanoparticles were calculated from the PXRD data. Energy-dispersive x-ray analysis confirmed the chemical homogeneity (49.88:51.12 at.%) of the samples. The effects of rotational velocity as well as mode of grinding on the morphology and the size of SnSe powders were investigated using electron microscopes. The direct optical transition with band gap varied from 1.75 eV to 2.28 eV was elucidated from UV-Vis-NIR data. Photoluminescence revealed an increase in the intensity of the emission peak at 462.97 nm with angular velocities for both types of grinding. The variation of electrical resistivity (36–107 Ω cm) and mobility (3.45–1.12 cm^2/Vs) with rotational speed was calculated for all the samples. The results obtained for the ball-milled nanoparticles pave the way towards the reduction of particle size, formation of stable morphology, and appreciable crystalline structure quality suitable for solar cell absorbers.

✉ A. G. Kunjomana
kunjomana.ag@christuniversity.in

[1] Department of Physics and Electronics, CHRIST (Deemed to be University), Bangalore, Karnataka 560 029, India

[2] Department of Physics, SES College Sreekandapuram, Kannur, Kerala 670 631, India

[3] Department of Physics, Nirmalagiri College, Kuthuparamba, Kannur, Kerala 670 701, India

[4] Department of Physics, St. Thomas College, Palai, Kottayam, Kerala 686 574, India

Graphical Abstract

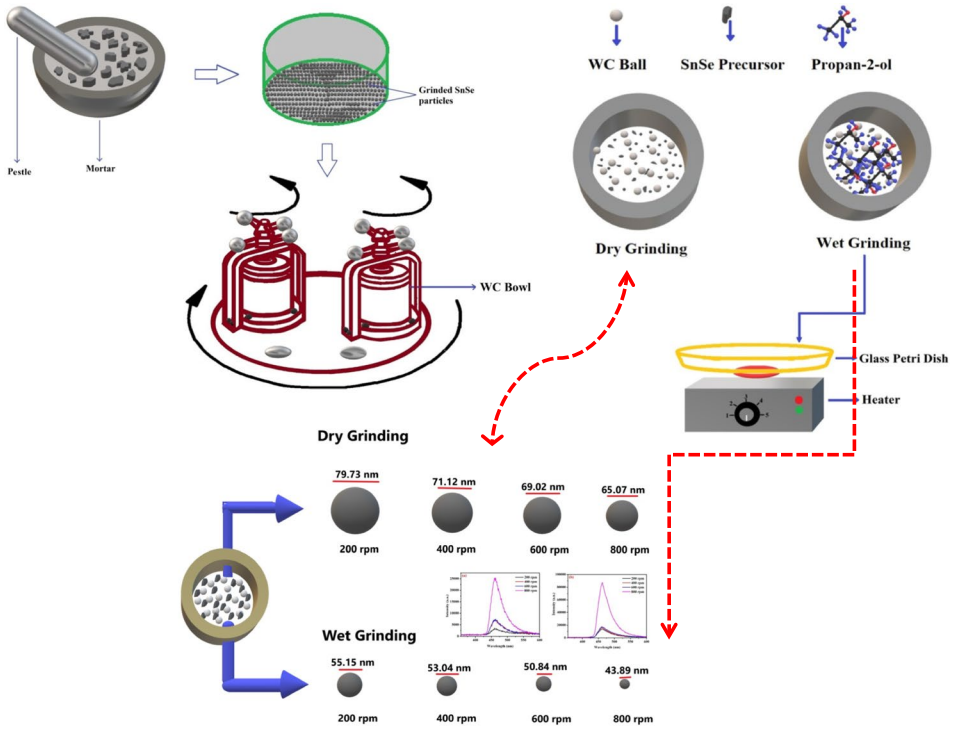

Keywords Tin monoselenide · ball milling · nanoparticles · milling rate · dry and wet grinding · physical property

Introduction

IV-VI semiconducting chalcogenide materials have gained tremendous interest over the past few decades due to their technological applications in areas including thermoelectric power, optical switching, photodetection, and optoelectronics.[1–5] In particular, tin monoselenide (SnSe) with excellent physicochemical properties has garnered immense attention, as it can be utilized as an efficient absorber material for solar energy harnessing.[6,7] SnSe crystallizes in an orthorhombic structure with unit cell parameters $a = 11.498$ Å, $b = 4.153$ Å, and $c = 4.440$ Å.[8] Apart from the excellent optoelectronic properties, the abundance, nontoxicity, and low environmental impact of the constituent materials are added advantages for commercial production.[9] In addition, the nanoscale synthesis of stoichiometric tin monoselenide samples is challenging and plays a pertinent role in the physical and chemical properties. Conventionally, the chemical route,[10] colloidal synthesis,[6] vapor transport deposition,[8] solvothermal method,[11] and ball milling[12] have been employed for the preparation of SnSe nanocrystals. Although the chemical method is feasible for the growth of nanoparticles, it involves complex procedures including the addition of toxic reagents. In chemical synthesis approaches, special care is required (e.g., chemical treatments, capping, doping) to harvest chemically pure nanosamples. Liu et al.[10] observed layered spiral-type nanoplatelets with helical periodicity on the surface of SnSe particles grown by the chemical route, which is undesirable for photovoltaic applications.[10] An attempt was made to grow good-quality SnSe nanosamples using the colloidal synthesis method, but it failed to produce stoichiometric samples with crystalline quality and involved complications due to several chemicals.[6] Although vapor transport deposition is an effective approach for producing single crystals of SnSe nanoplates, it is an intricate phenomenon involving ultrapure argon gas.[8] Advanced techniques like the low-temperature solvothermal route are expensive and induce extraneous traces of particles or contamination.[11] Therefore, these methods lack feasibility for the large-scale growth of nanomaterials. SnSe nanoparticles were also developed through mechanochemical synthesis in an argon atmosphere, and the studies revealed the presence of agglomerated selenium with thick clusters of unreacted Sn/Se.[12] The authors also observed the absence of an absorption edge using ultraviolet–visible (UV–Vis) analysis.

Of all the above growth methods, the top-down approach of materials through high-energy ball milling is found to be

superior, as it is facile and offers an ambient environment with reproducibility and high yield.[13] SnSe compounds are prepared using the dry mixing of the individual elements Sn and Se by ball milling as reported by Nee et al.[14] When these elements are mixed using the physical approach, it is very difficult to obtain nanocrystals with good quality, crystallinity, and stoichiometry, due to the utilization of elemental tin and selenium. On the other hand, in the present work, the initial stoichiometric precursors were prepared by the melt–mixing approach.[7,15] This primary precursor was further utilized for the ball-milling process in a systematic manner by carefully adjusting the mode of rotation and rotational speed. As such, the reports pertaining to the physical properties of stoichiometric SnSe nanosamples by dry and wet grinding are scarce. Hence, the present work focuses on the detailed investigation of the structural, compositional, morphological, optical, and electrical characteristics of mechanically produced SnSe nanoparticles.

Experimental

High-purity Sn and Se (99.999%) elements were taken in a specially designed quartz ampoule 100 mm in length, and with an inner diameter of 10 mm. The crucibles were thoroughly cleaned using soap solution, sulfuric acid, distilled water, and ultrasonic waves in order to avoid traces of extraneous particles.[15] For the preparation of the SnSe charge, the ampoule containing the materials was sealed under high vacuum (10^{-6} mbar), placed in a muffle furnace, and gradually heated to stabilize at 880°C for 48 h. Periodic rotation (angular velocity = 60 rpm) followed by slow cooling helped in achieving the stoichiometric SnSe compound. Mechanical synthesis of SnSe powders was then performed in a planetary ball milling unit (FRITSCH Pulverisette 7) using the physically distinct ingot. Two tungsten carbide (WC) vials, 45 cm^3 in volume ($V = \pi r^2 h$; r and h are the radius and height of the vial, respectively), filled with 200 WC balls, 5 mm in diameter, were used as the milling bodies. The customized SnSe charge (10 g) ground with the aid of a mortar and pestle was used as the precursor for the milling process (Fig. 1). In order to avoid external contamination, the WC chambers were air-tightened by Teflon rings and locked using spindle clamping devices. The formation of nanoparticles depends on factors including the material of the balls, speed and type of grinding, and ball-to-powder weight ratio.[16,17] During wet mode, 5 ml of isopropyl alcohol was added to the powdered precursor. The milling time was programmed to 20 min in both cases and the chambers were closed during all the experiments. The problems related to excess heat formation and pinning of balls to the sides of the container at high angular velocities were addressed by adopting reverse rotation as well as 1 min pause during each 10 min. Thus,

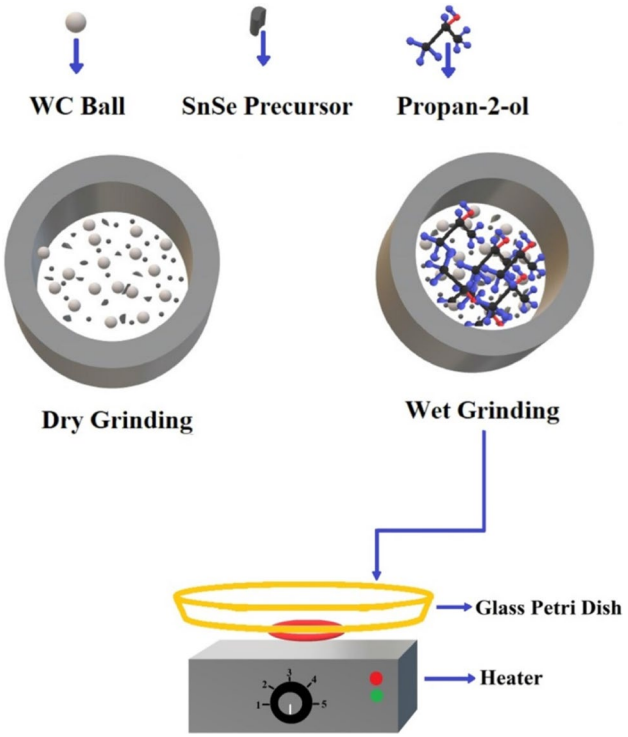

Fig. 1 Schematic representation of the SnSe nanoparticle preparation route.

the novel synthesis procedure helped to maintain a balanced operation atmosphere for the production of SnSe nanocrystals. A small quantity of the sample (1 g) was taken out of the bowl at regular intervals for further characterization.

X-ray diffraction with CuKα radiation facilitated structural analysis of the nanoparticles. The profiles were recorded from 10 to 80° angular range at a scanning rate of 0.05° (2θ). The single crystalline nature of the grown SnSe nanoparticles was verified using a selected area electron diffraction (SAED) pattern. Compositional details of the prepared materials were examined by energy-dispersive x-ray analysis (EDAX) with a silicon drift detector (SDD). Morphology and particle size were analyzed with the aid of scanning electron microscopy (SEM, Zeiss Ultra-55) at an accelerating voltage of about 20–30 keV. Prior to the characterization by high-resolution transmission electron microscopy (HRTEM, JEOL JEM-2100) operated at 230 keV, the samples were immersed in isopropyl alcohol and ultrasonically deagglomerated (IDS Ultrasonic Cleaner C-4820 with 42,000 Hz frequency) to separate clusters into individual nanoparticles. ImageJ software was utilized to calculate the average particle size and identify diffraction spots obtained in the SAED pattern. Band gap studies were performed in the wavelength range of 200–3000 nm, by employing an ultraviolet–visible–near infrared (UV-Vis-NIR) spectrophotometer (Varian Cary 5000). At room temperature, a Fluorolog-3

spectrometer was used to record the photoluminescence (PL) spectrum at an excitation wavelength $\lambda_{ex} = 360$ nm. The electrical properties of the prepared samples were probed via the van der Pauw technique and Hall effect experiment (Polytronic Research Electromagnet HEM-150).

Results and Discussion

The properties of compounds rely on the internal atomic arrangement, imperfections, etc., which are predominantly affected by the synthesis protocols. Particle size reduction is one of the most important steps for the enhancement of optoelectronic properties towards photovoltaic applications. In this regard, ball milling is considered a facile physical method for the preparation of nanosamples. A unique feature of the planetary mill is the suitability for the dry and wet comminution of hard, brittle, and fibrous materials. Hence, this is an appropriate choice for the production of nanomaterials at a short interval of time.[17] The current research paper focuses on two modes of mechanical synthesis, dry and wet grinding. Here, the applied force is sufficient to disperse the initial microscale materials into atomic-scale agglomerates, maintaining a stoichiometric balance. Contamination from the equipment is a crucial problem associated with the grinding of powders, which adversely affects the optoelectronic properties. Herein, tungsten carbide balls and bowls were introduced, as tungsten has high density (15.63 gcm^{-3}) compared to tin monoselenide and leads to increased impact energy of the collision, facilitating the production of one-dimensional samples.[18] A schematic of the synthesis route adopted in the present work is depicted in Figs. S1 and 1. During this process, the powders of SnSe undergo dramatic shear and stress from the milling media, which enables the reduction of particle size.[19] The powder was subjected to repeated interactions with the milling balls until the samples achieved a characteristic length on the order of a few nanometers. In planetary ball mills, the comminution of the sample material takes place primarily through the high-energy impact of grinding balls. To prepare the nanoparticles, the grinding bowl containing the material to be ground using grinding balls rotates around its own axis on a main disk rotating in the opposite direction. The overlapping of the centrifugal forces causes the sample material and grinding balls to bounce off the inner wall of the grinding bowl during the process. The grinding balls cross the bowl diagonally at an extremely high speed and grind the sample material on the opposite wall of the bowl. The bowls reach approximately twice the speed of the main disk during milling.

Powder x-ray diffraction (PXRD) has been considered the fingerprint technique for the elucidation of crystallographic features like position, intensity, and width of the diffraction lines.[20,21] Figure 2 represents the x-ray diffractograms of the prepared SnSe nanosamples. The PXRD pattern confirmed that the synthesized materials possess an orthorhombic crystal system without the presence of any peaks of other impurities such as carbon, tungsten, or oxygen. The SnSe phase was oriented along the (111) crystal plane at an angle

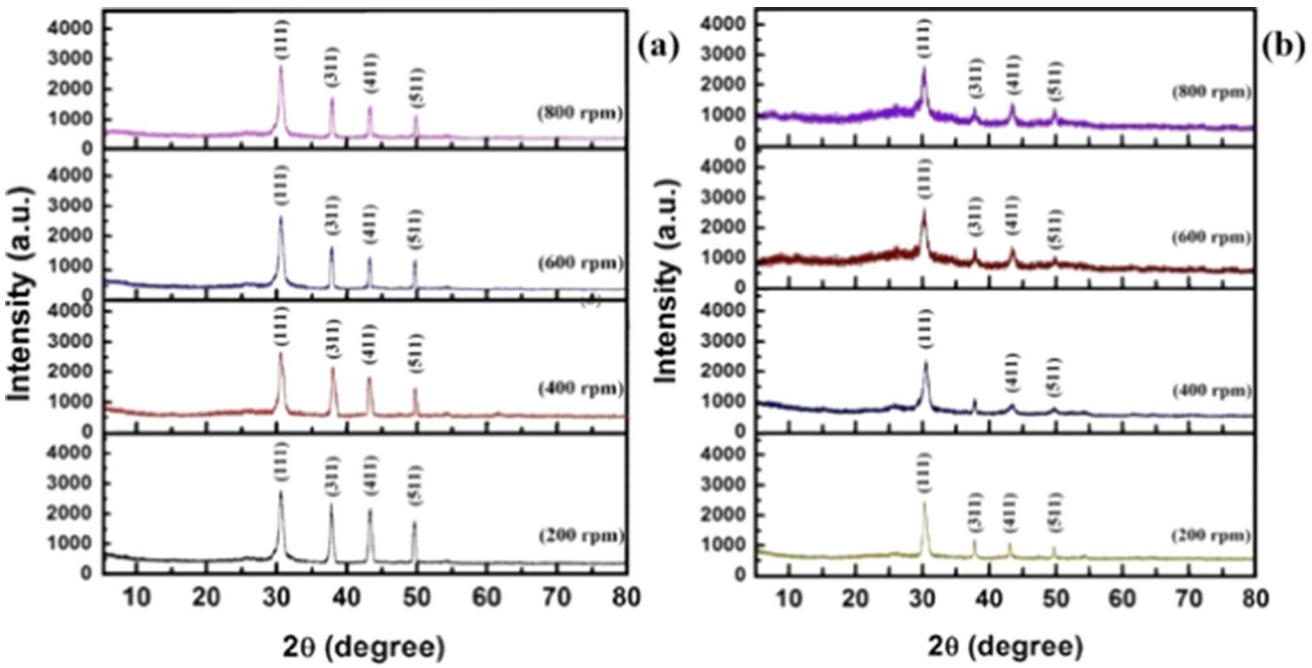

Fig. 2 Effect of ball milling on XRD profiles obtained for (a) dry and (b) wet grinding.

of 30.50°. The intense (111) plane arises due to the mutual reinforcement of atoms from a large number of similar parallel planes.[21]

Achimovičová et al.[12] detected traces of un-reacted Sn and Se peaks for mechanochemically ball-milled SnSe samples. The appearance of elemental materials in the XRD profile was due to the partial conversion (83%) of Sn and Se during mixing, pulverizing, and chemical reaction leading to the final compound. These authors also noted poor scattering intensity of the ball-milled tin monoselenide. This result was an indication of improper arrangement of atoms, inhomogeneity, structural instability, and incomplete reaction of Sn and Se. To prevent such problems, the stoichiometric SnSe precursor was synthesized by employing a constant-temperature muffle furnace and powdered to micrometer size before the ball-milling process, which helped to avoid the complex steps associated with the mechanochemical method. Figure 2a shows the PXRD pattern of the SnSe nanoparticles prepared via dry grinding at a rotational speed $R_s = 200$ rpm, in which (111), (311), (411), and (511) planes were observed. The sharp and strong peaks were indexed to the orthorhombic system as per the standard ICSD XRD data for SnSe (PDF number: 01-075-1843 48-1224). The cell dimensions were calculated from the PXRD data as $a = 4.435$ Å, $b = 11.498$ Å and $c = 4.148$ Å, matching well with previous works.[7] When the rotational speed of the ball mill was increased from 200 rpm to 800 rpm in steps of 200 rpm, a successive reduction in the intensity of peaks was observed in the PXRD profiles. The decrease in intensity of the peaks at higher R_s is due to the successive reduction in the degree of crystallinity. The up-shift of the XRD peaks was not detected in the present research work, which ensures the absence of compressive strain in the SnSe nanoparticles during the milling process. On the other hand, Giri et al.[22] observed structural changes, compressive strain, decreased crystallinity, and isotropic strain on ball-milled ZnO nanocrystals. However, the peak widening of the SnSe nanopowders (Fig. 2b) in wet milling conditions is much greater than that in dry grinding (in the presence of isopropyl alcohol [IPA]). This is an expected observation since conditions employed during dry milling are more severe than those during wet milling. In other words, most of the kinetic energy generated by the ball-to-ball and ball-to-vial collisions is absorbed by the liquid media during wet milling as opposed to dry milling, where almost all kinetic energy is directly transferred to the powders. As a consequence, it was observed that the crystallinity of the dry-milled powders has to be much smaller than those milled in wet conditions. Careful experimentation helps to avoid the extraneous elements (Fig. 2), there was a high probability that the emergence of peaks such as W, C, and O from the milling media (vial and balls) owing to the excessive impact energy accumulated during milling at a high rotational speed. Besides, the SnSe nanocrystals were produced using a low-temperature chemical route with the addition of sodium to ensure the quality of the SnSe.[11] Researchers explained that the longer reaction time led to serious agglomeration and larger grain size. In order to synthesize defect-free, dislocation-less, and structurally stable SnSe nanoparticles, careful elimination of the inert atmosphere with normal and reverse rotation under a proper interval of time was adopted.

In order to further reduce the particle size, the grinding was shifted to wet mode by adding a small amount of solvent medium (propan-2-ol). This assisted in eliminating the mechanical and structural damage that occurred during milling at a high rotation speed (600–800 rpm). PXRD profiles of the wet-ground samples confirmed the absence of traces of peaks due to the accumulation of the external medium (Fig. 2b). Hence, these results show the complete evaporation of propan-2-ol from the harvested powder products due to the 10-min resistive heating (Fig. 1). Also, with enhancement in R_s, the full width at half maximum of the orientation plane was increased, accompanied by a reduction in peak intensity, which shows the reduction in particle size.

The chemical composition of a compound plays a vital role in its optoelectronic properties. Considering this, EDAX is a widely used technique for the identification of elements present in the compound, which is used to probe the quality and chemical homogeneity of the synthesized nanoparticles. The EDAX spectra of SnSe nanoparticles synthesized through both dry and wet grinding at different milling speeds are presented in Fig. 3. Contamination arising due to carbon (C) and tungsten (W) used as bowls/balls during the milling process was eliminated by the 10 min rotation (clockwise) of the jar followed by 1 min pause and anticlockwise 10-min spin. EDAX (atom %) investigations of the nanoparticles confirmed the correct Sn:Se chemical composition without the presence of extraneous elements. Elemental analysis revealed that the samples were nearly stoichiometric with negligible change ($\sim \pm 0.05\%$) from the standard proportion due to the strong interaction between the particles and balls during comminution. Conversely, Franzman et al.[23] reported the atomic ratio of SnSe nanocrystals synthesized through the solution-phase method as 48.1:59.9 at.%, where EDAX and x-ray photoelectron spectroscopy (XPS) confirmed the presence of carbon (C), nitrogen (N), oxygen (O), and sulfur (S). These impurities arose from the use of several chemical reagents including $C_{12}H_{27}N$, $C_{12}H_{26}S$, and $C_8H_{18}Se$. Jahangiri et al.[24] reported that titanium powder particles fabricated during mechanical alloying in IPA were smaller and more homogeneous than those milled in ethanol. Considering such factors, in the present work, isopropyl alcohol is used as a medium for wet grinding instead of ethanol to avoid oxygen contamination. On the other hand, studies on ball-milled tin monoselenide particles were carried out by Chen et al.,[25] and the presence of carbon, oxygen, and copper were detected

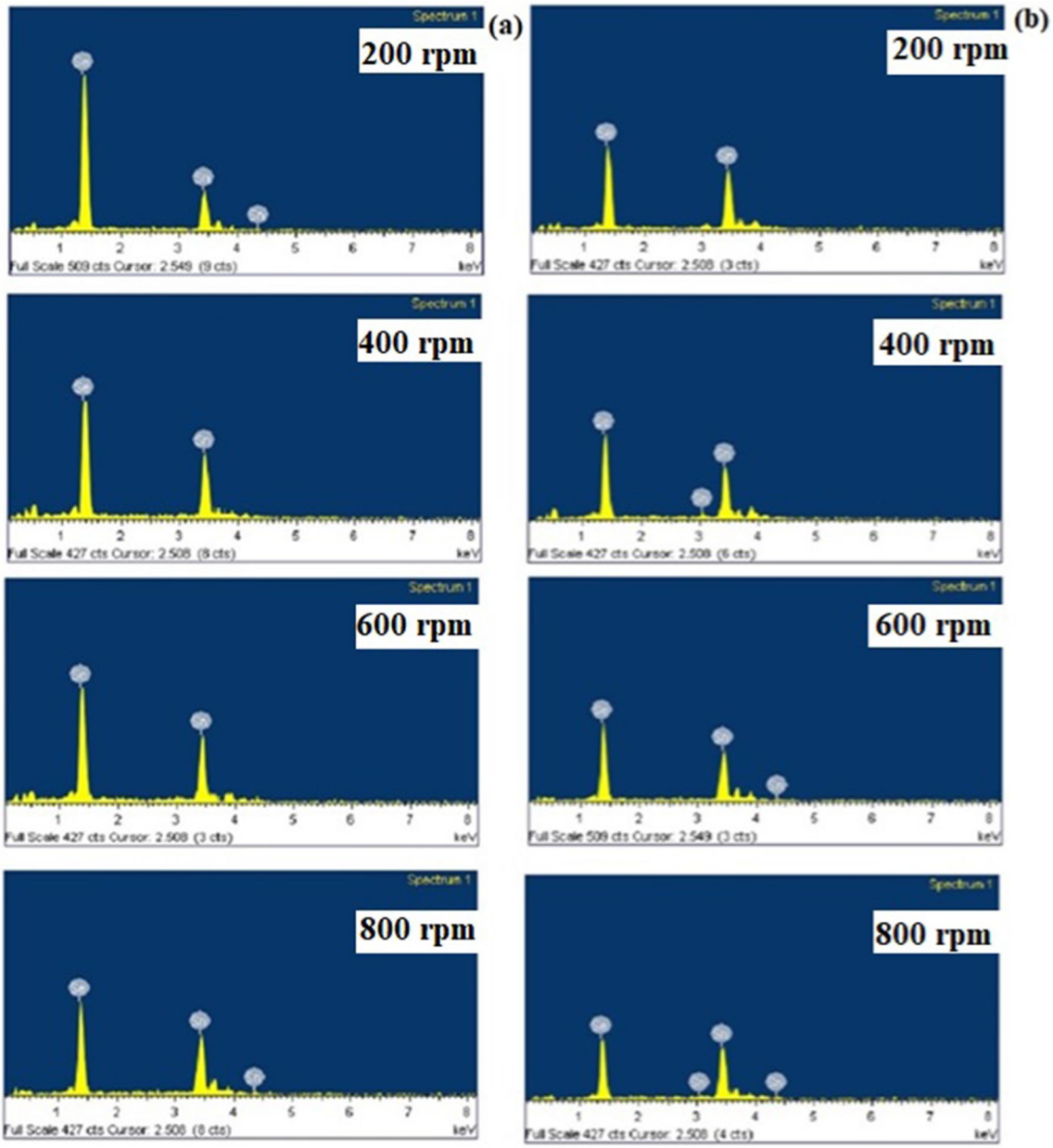

Fig. 3 EDAX spectra of (a) dry- and (b) wet-ground SnSe nanoparticles.

from the energy dispersive spectroscopy (EDS) spectra. Thus, the PXRD and EDAX results reveal that the nanocrystals grown via high-energy ball milling comprise a single phase, confirming that the right stoichiometric proportion of constituent elements was used. The result is further supported by the PXRD (Fig. 2a, b).

Transmission electron microscopy (TEM) is one of the conventional methods for the determination of induced morphologies in the sample along with its particle size.[22] Herein, a high-resolution transmission electron microscope is utilized to reveal narrow features of the microstructure. Figure 4 mirrors the influence of both dry and wet grinding on the quality of the acquired products. Results showed a substantial reduction in the sample dimension to the nanometer regime.

In the case of dry grinding, at lower angular velocity (200 rpm), it is clear that the nanoparticles exhibited a high tendency to form clusters (Fig. 4a). In order to overcome the challenges associated with the aggregation of nanopowders, the milling rate was purposively increased in successive steps. When $R_s = 800$ rpm, a slight reduction in the agglomerated nanoparticles was observed (Fig. 4b). However, the presence of thick clusters of unreacted Sn- or Se-rich amorphous phase was detected using TEM analysis on SnSe

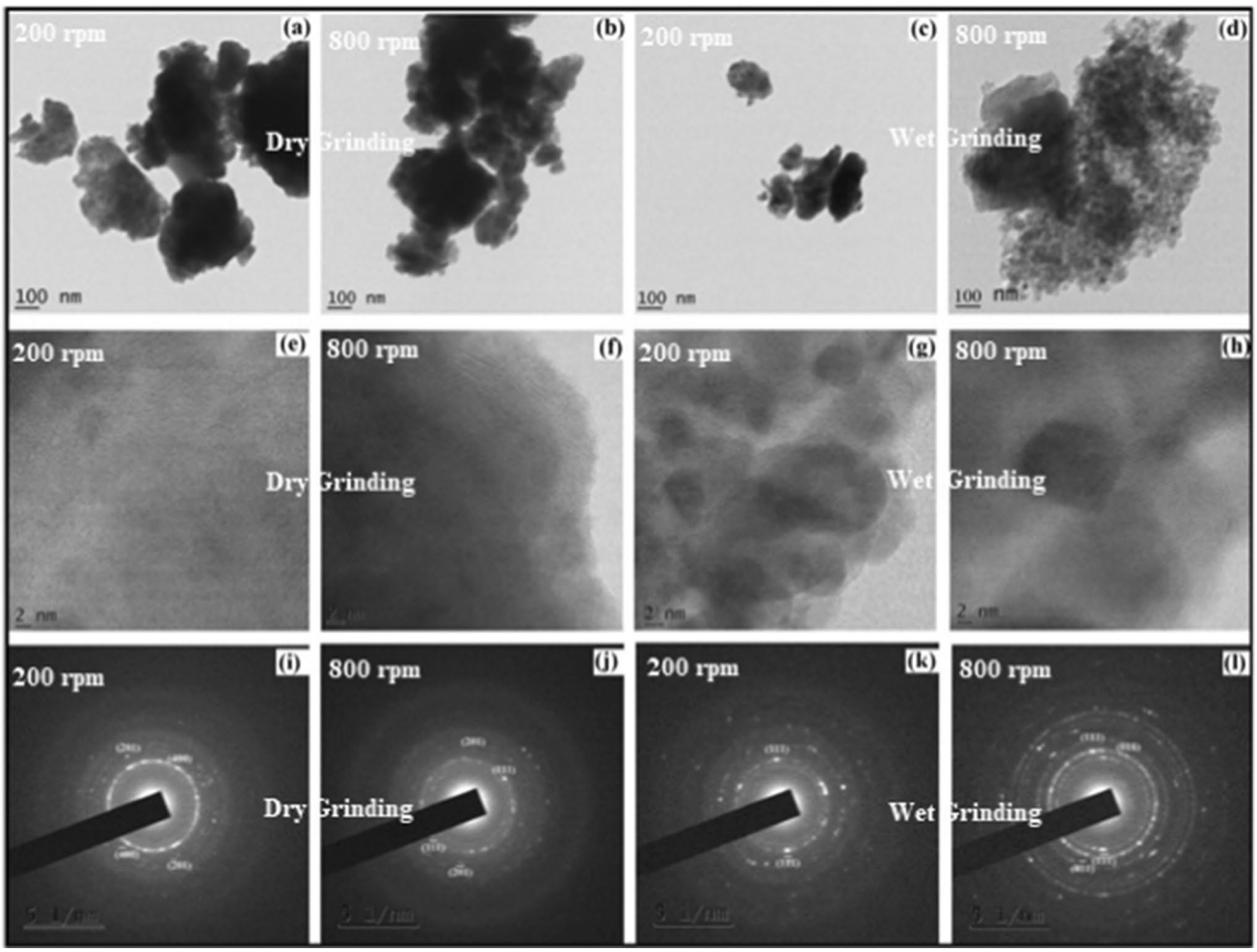

Fig. 4 (a–d) TEM image of SnSe nanocrystals grown via dry and wet grinding at 200 and 800 rpm (e–h) HRTEM image of SnSe crystals prepared dry and wet grinding (i–l) SAED pattern of the SnSe nanopowder synthesized through dry and wet grinding.

crystals prepared using mechanical alloying.[12] Even though the latter have idiomorphic shapes with length of 80 nm, the samples exhibited low angle tilt boundaries. Tiny crystals formed were round in shape, and the larger ones appeared as square-like. In order to further reduce the size of the SnSe samples within the experimental constraints, the rotational speed was varied from 200 rpm to 800 rpm. Figure 4e and h shows the HRTEM images of SnSe nanoparticles synthesized through dry grinding at 200 rpm and 800 rpm, respectively. However, dry grinding at high R_s failed to achieve a stable morphology, and therefore it is not a suitable choice to produce uniform surface topography with finer particle size reduction. Hence, a wet-grinding approach was introduced with the addition of 5 ml of isopropyl alcohol to the nanopowder precursor. Figure 4g depicts the round nanoparticles (piled together) obtained from wet mode at $R_s = 200$ rpm. When R_s was elevated from 200 rpm to 800 rpm, the surface morphology of tin monoselenide maintained the same trend with reduced pile-up of particles as evident from Fig. 4h. During wet grinding, the large strains on SnSe powders enabled the reduction in particle size, but the solution medium helped to reduce the defect formation due to collisions. These results pave a new path for the development of stable nanoscale morphological formation through the ball-milling technique. The ball-milled nanoparticles ($R_s = 200$ rpm) possessed clear lattice fringes with an interplanar spacing of 0.29 nm assigned to the (111) plane of SnSe orthorhombic crystal structure (Fig. 4i). The mean size of the particles synthesized through dry grinding varied between 75.16 nm and 63.39 nm. Furthermore, attempts to disperse powders more uniformly by the addition of isopropyl alcohol were successful, suggesting that the clusters are due to the weak surface bonding, which is formed under high pressure developed during milling. In the case of wet grinding, as the rotational speed increased from 200 rpm to 800 rpm, the average particle size reduced from 53.35 nm to 35.11 nm. It is interesting to note that the morphology of SnSe quantum dot colloids prepared via irradiation bear a resemblance to

the samples milled at $R_s = 800$ rpm.[26] Selected area electron diffraction (SAED) associated with TEM analysis helps to evaluate the degree of crystallinity. SAED patterns (Fig. 4i, j) of SnSe nanoparticles prepared at 200–800 rpm through dry grinding show well-defined diffraction patterns, confirming the polycrystalline nature of the SnSe nanoparticles. These patterns match with the obtained PXRD data as well, showing the polycrystalline nature of the synthesized particles. When R_s was enhanced from 200 rpm to 800 rpm (dry grinding), the brightness of the diffraction spots was reduced (Fig. 4i, j). Figure 4k and l show the SAED patterns of the nanoparticles prepared using wet grinding at $R_s = 200$ and 800 rpm respectively. Here, the circular rings were intensified and increased in number along with increased angular velocity (Fig. 4k, l). The lower particle dimension is also evident from HRTEM and FESEM images. As grains in a polycrystalline material show all orientations comparable to the pattern obtained from single-crystal rotation, the ring formation from the SAED pattern is equivalent to the rotation of a single crystal around the axis of the transmitted electron beam. When the selected area includes many individual small crystals, it can also lead to the formation of rings in the SAED pattern.[21] Diffraction spots in the SAED trace are indexed to orthorhombic SnSe in accordance with the reported literature.[10]

Scanning electron microscopy (SEM) is useful to unearth the microscopic structure of samples up to a few nanometer ranges, thereby exploring the growth mechanism, size, particle distribution, and defect formation. Higher magnification, larger depth of field, etc. are some of the fundamental factors that make SEM an indispensable tool for the morphological characterization of the material.[27] In the present study, field emission scanning electron microscopy (FESEM) is exploited for capturing the minute microstructural development of the nanocrystals. Figure 5 depicts the FESEM micrographs of SnSe nanoparticles obtained through dry and wet grinding, respectively.

Figure 5a–d clearly shows that the ball-milled SnSe nanosamples obtained through dry grinding consisted of aggregated particles with irregular shapes and sizes. When the milling rate was 200 rpm, the powders tended to agglomerate, which can be attributed to the large specific surface area. Similar results have been reported for ternary selenide materials such as $CuInSe_2$ grown through mechanical production. Herein, the rotational speed was programmed to 550 rpm, and a tungsten carbide milling chamber (250 ml in volume) consisting of 50 balls (10 mm in diameter) was used for this process. The authors obtained a particle size of only 200 nm even after 60 min of milling.[13] However, in the present work, the average size of the SnSe powders was calculated to be less than 80 nm from the SEM image (Fig. 5a) obtained for the dry-ground sample at 200 rpm. The high-density WC bowl (45 ml), small-diameter balls (3 mm) and longer time (20 min) of rotation (clockwise as well as anticlockwise) during the growth period helped in reducing the dimension of the particle to the nanoscale range. When R_s was increased to 400 rpm the particle size was further reduced, but the surface microstructure remained to be constant (Fig. 5b). In order to reduce the particle size to less than 50 nm, the angular velocity of the WC growth tank was slightly enhanced to 600 rpm and 800 rpm. However, this attempt failed in producing samples of the target size (Fig. 5a, b). In general, particle size decreases with an increase in milling speed. The rate at which the milling balls move enhances with rotational speed. This also increases the average mean free distance of a single powder colliding with the ball. Thus, as the size of the vessel is fixed, the collision frequency of the powder increases. Hence, when the milling rate was further increased from 200 rpm to 800 rpm, the particles were further compressed,[28] and together with the larger grains, the presence of very fine particles occurred. Even though agglomerates are formed, fine particles belonging to the nano region are retained. The conclusions drawn from the dry-ground samples motivated the search for a new strategy to scale down the particle dimension. Hence, in the current research wet grinding is adopted to achieve particle size reduction and uniformity. Herein, isopropyl is utilized as the solvent media for further attrition. The high vapor pressure of isopropyl alcohol at room temperature, its availability, and the ability to not contaminate the SnSe precursor or WC balls/bowls during the synthesis process make it suitable to act as the wet grinding medium. Isopropyl solution also helps in reducing the structural and mechanical damages due to the collision during crushing. Figure 5e shows the SnSe nanoparticle having an average size of ~55 nm grown at $R_s = 200$ rpm. To further reduce the particle size and mold the powder shapes of the grown samples, the rotation velocity was increased to 400 rpm and 600 rpm (Fig. 5f, g). The nanoscale morphological developments are revealed by the FESEM image (Fig 5h). The SnSe particle distribution was found to be quite uniform, and the nanopowders exhibited spherical morphology. Also, the average sizes of the as-milled specimens were found to be reduced. The new version of ImageJ software was utilized to measure the particle size with the help of FESEM images, and the average value is presented in Fig. 6. The average particle size of SnSe powders via dry grinding varied from 79.73 nm to 65.07 nm (Fig. 6a) and that of the powders obtained through wet grinding varied from 55.15 nm to 43.89 nm (Fig. 6b). Graphical representation of the particle size versus rotational speed via dry and wet grinding is depicted in Fig. 6a and b. To the best of our knowledge, we are the first research team to explore the nearly linear relationship between particle size and angular velocity. These results provide a novel synthesis strategy for the downscaling of particle size using ball milling.

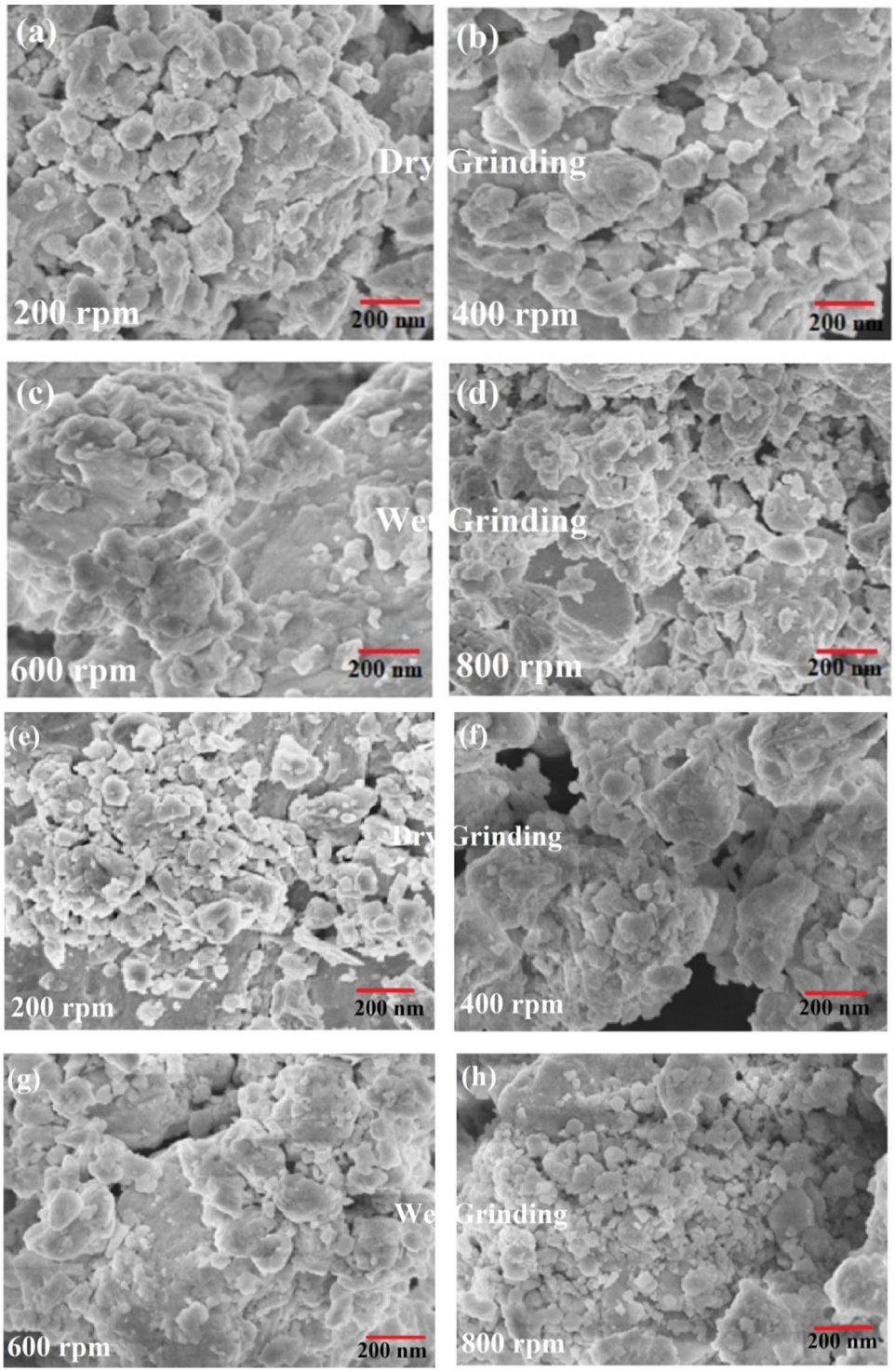

Fig. 5 FESEM images of SnSe: (a–d) dry attrition and (e–h) wet attrition with varying milling rates from 200 to 800 rpm.

A UV-Vis-NIR spectrophotometer was equipped to investigate the optical properties of the obtained sample. Herein, the absorption spectrum was recorded in the wavelength range from 200 nm to 3000 nm. The optical absorption coefficient (α) and the energy of light ($h\nu$) vary according to the relation:

$$(\alpha h\nu)^2 = A\left(h\nu - E_g\right) \quad (1)$$

where A is an arbitrary constant, E_g is the band gap, and h is Planck's constant. Figure 7a and b show the obtained Tauc plot for the SnSe nanoparticles obtained via dry and wet grinding. From the plots, it is clear that the band gap

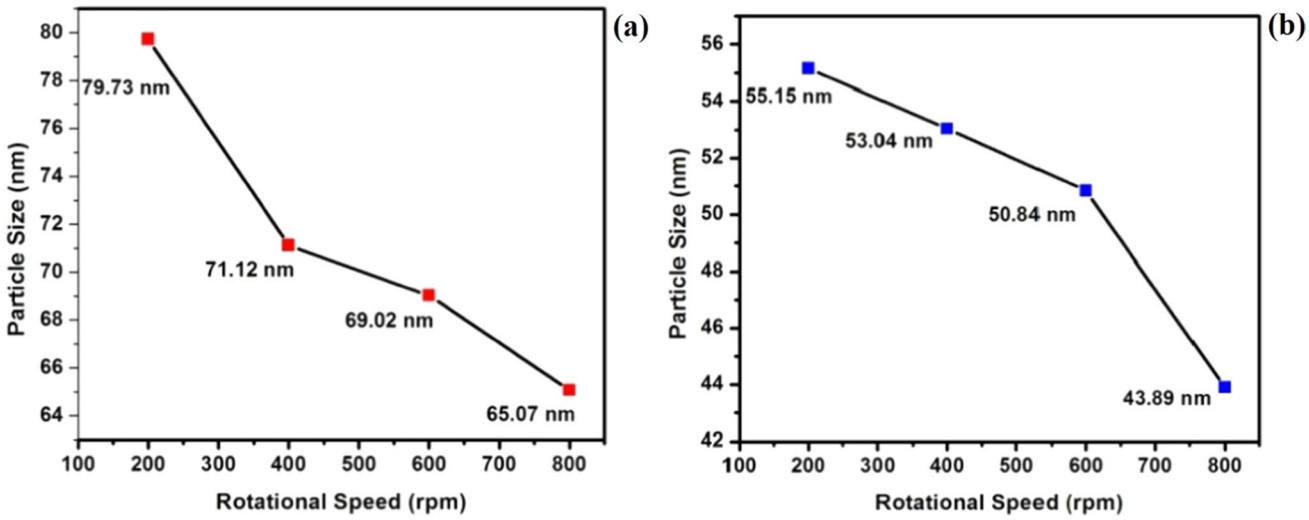

Fig. 6 Plot of rotational speed versus particle size of the ball-milled SnSe nanoparticles via (a) dry and (b) wet comminution.

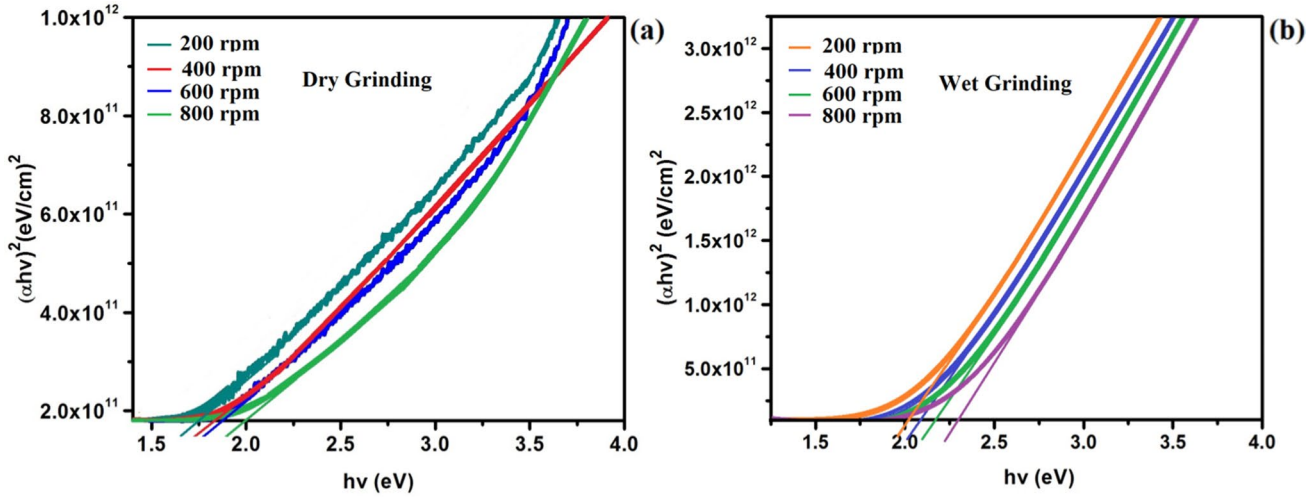

Fig. 7 Plot of $(\alpha h\nu)^2$ versus photon energy for the samples obtained via (a) dry and (b) wet grinding.

increases as the milling rate is enhanced. The variation of the optical band gap with respect to milling speed is presented in Table SI (Supplementary Information). As the attrition rate increased from 200 rpm to 800 rpm, the particle size was further decreased thereby increasing the bandgap from 1.75 eV to 2 eV. Further enhancement in bandgap is due to the increase in the surface-to-volume ratio as the particle size is reduced.

Furthermore, during wet milling, when the rate of grinding increases, the particle size decreases, resulting in the enhancement of the energy gap (2.02 eV to 2.28 eV). This can be attributed to the quantum confinement effect, wherein electrons and holes of the nano-size semiconductors are confined to a smaller particle radius.[29] The samples with size of a few nanometers have a larger band gap, and hence the radiation from these particles is shifted to lower wavelengths.[30] Therefore, in general, the band gap can be tuned with the aid of crystallite size. Similarly, SnSe nanosamples were synthesized by a planetary mill, and studies on optical properties were carried out. No absorption edge was observed from the spectra of mechanochemically synthesized SnSe samples.[12] Studies on the colloidal synthesis of SnSe nanocrystals were reported by Baumgardner et al.,[6] in which the authors found that the samples had both direct and indirect band gaps. Confinement effects in the samples and the size-dependent trend in energy were also discussed.

Room-temperature photoluminescence (RTPL) is an indispensable technique used for the exploration of optical properties of the obtained nanosamples. The excitation photon wavelength, $\lambda_{max} = 360$ nm is absorbed by the SnSe

nanoparticles and imparts excess energy to the material in a process called photoexcitation. The way of elimination of the absorbed energy is termed luminescence. So, the photoluminescence of the ball-milled nanoparticles is the spontaneous emission of light from the material under optical excitation. The amount of light emitted is related to the relative contribution of the radiative process. PL spectroscopy helps to capture the information only on the low-lying energy levels of the investigated system. The radiated photons from the conduction band of the mechanically synthesized SnSe powders were collected using the detectors, and the obtained emission spectrum is presented in Fig. 8a and b.

The PL profile appeared to be in the range of 360–600 nm and the emission spectrum showed the presence of only a single intense peak at 462.97 nm for both dry and wet grinding. A similar kind of PL profile was reported on the colloidal SnSe quantum dots and exhibited blue photoluminescence at 420 nm. The high energy shift in the PL spectrum of the samples was due to the quantum confinement effect.[26] On the other hand, the PL profile of the SnSe nanosheets obtained through aqueous phase one-pot green synthesis was a convolution of two bands, i.e., Band-I at 420 nm and Band-II at 470 nm. Emission of the absorbed energy during the transition of an excited electron from the unstable conduction band to the equilibrium stable state in semiconductors also involves localized defects or impurity levels. Therefore, analysis of the PL spectrum leads to the identification of specific dislocations, and the magnitude of the PL signal allows us to determine their concentration.[31] However, in the currently synthesized sample, shoulder peaks were not observed, which confirms the absence of defects or dislocations, etc., in the nanopowder. As the size of SnSe nanocrystals decreased, absorption increased, which leads to a blue shift in the photoluminescence spectra towards shorter wavelengths and high intensity.[13] This is due to the band emission from several small nanocrystalline clusters. When the rotational speed was enhanced through dry grinding, a reduction of the SnSe particle size to few nanoscales occurred, which intensified the PL emission as is evident from Fig. 8a and b. Hence, these PL results reveal that the magnitude of the light emission intensity of SnSe nanoparticles was amplified confirming the high quality of the prepared nanopowder. From the PL results obtained, one can conclude that the intensity of the emission profiles was enhanced along with the size reduction and stable morphology of the nanoparticles. The increased intensity is due to the high absorption of the photon and surface-to-volume ratio enhancement, which is the core reason for the amplification of the absorption of light.

In order to probe the electrical parameters like resistivity, mobility, etc. the collected SnSe powders were pelletized with 1 mm length and 1 mm thickness as shown in the inset of schematic Fig. 9a. Despite the progress in SnSe semiconducting materials and devices, there are numerous technological challenges associated with good-quality tin monoselenide samples and the fabrication of an efficient device. The selection of compatible, low-resistant, and thermally stable ohmic contact is inevitable to unearth the precise electrical properties of the prepared sample. In this regard, Au was selected as a contact electrode, which has low resistance, less chance for contamination, and high thermal stability. The four Au fingers were deposited on SnSe pellets for the contact to measure the electrical parameters with the assistance of the thermal evaporation method under 2×10^{-6} mbar vacuum atmosphere. This will help avoid the presence of impurities during the deposition. When the angular velocity of the bowl was increased on both dry and wet grinding, the electrical resistivity was enhanced,

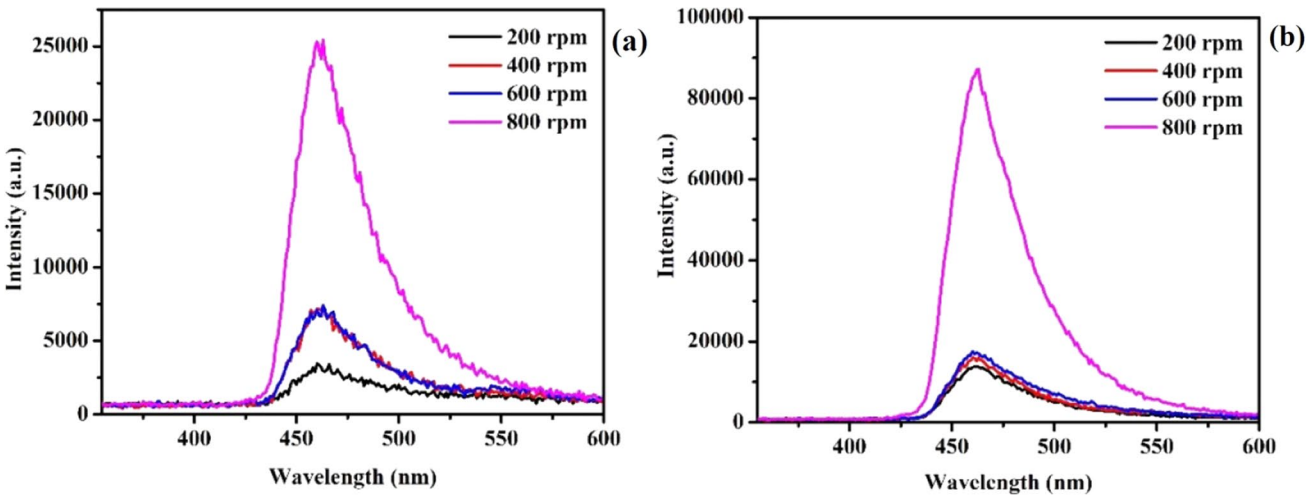

Fig. 8 Photoluminescence spectrum of SnSe nanosamples by (a) dry and (b) wet grinding.

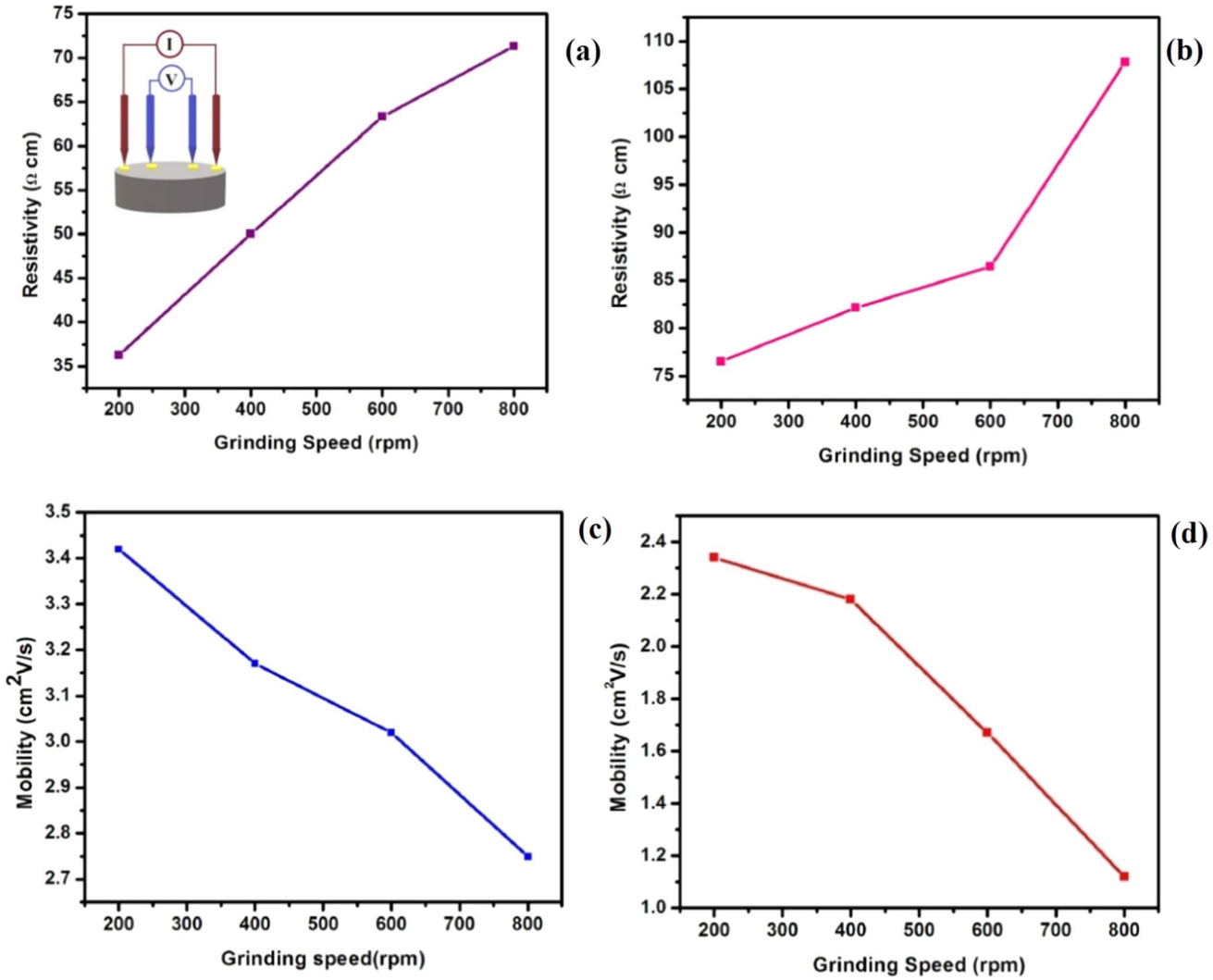

Fig. 9 Plot of resistivity versus angular velocity for (a) dry and (b) wet grinding; Graphical representation of mobility versus rotational speed for (c) dry and (d) wet comminution.

as depicted in Fig. 9a and b. The increase in resistivity is due to the distortion of crystallinity and the aggregation of grain boundaries. The agglomerated grains will be the active center for the scattering of electrons as well as the capture of electrons during carrier movement; this will increase the electrical resistivity and decrease the mobility. Chen et al. reported that SnSe and potassium-doped SnSe nanocrystals synthesized by ball milling showed enhanced electrical conductivity and sinusoidal variation in mobility with respect to milling time (5, 8, and 12 h).[25] However, in the present work, a trend toward gradual enhancement of electrical resistivity and a slow decrease in mobility were observed when the angular velocity of the grinding jar was increased from 200 rpm to 800 rpm. These changes were clearly visible from the graphical representation (Fig. 9c, d). *P*-type conductivity and the variation in electrical conductivity have also been reported in the literature.[32] The positive value of the Hall coefficient and hot probe experiments confirmed the *P*-type conductivity. The increases in resistivity with rotational speed (reduction of particle size) during the ball-milling process in both dry and wet grinding were presented in Table S1 (Supplementary Information).

Conclusions

In this research work, nanosized SnSe powders were synthesized by dry and wet grinding (with the addition of propan-2-ol) through high-energy planetary ball-milling. Special care was taken to eliminate the presence of impurities in the milled SnSe nanoparticles by using customized stoichiometric precursor material. EDAX analysis confirmed the chemical homogeneity (49.88:51.12 at.%) of the obtained nanoparticles. Morphological modification,

particle size, and agglomeration were investigated utilizing FESEM and HRTEM images. Particle size was greatly influenced by the milling speed and the grinding mode. The average particle size was calculated in the range of 20–80 nm using ImageJ software. The slight distortion in the intensity of the peaks as well as the widening of the peak width was observed when the milling speed was varied from 200 rpm to 800 rpm at both dry and wet grinding. The transition of partial crystalline nature to the polycrystalline structure was clearly visible from the PXRD and SAED patterns. The absorption characteristics of the obtained SnSe nanoparticles were investigated through UV-Vis-NIR spectra and revealed an optical band gap in the range of 1.75 eV to 2.28 eV, this wide band gap is due to the high surface-to-volume ratio and quantum confinement effect. RTPL results gave evidence for the enhanced surface-to-volume ratio as the rate of milling increased, and it was further increased during wet grinding. The emission intensity of the SnSe nanoparticle was observed to be increased along with the milling speed and the mode of grinding. Hence, the synthesized SnSe nanoparticles were found to hold appreciable structural, morphological, optical, and electrical properties, thus this binary chalcogenide semiconductor in nanoform is promising as an absorber material for solar cell applications. In the current research work, we attempted to reveal the morphological, atomic arrangement of crystal, and optoelectronic properties of SnSe nanoparticles by dry and wet grinding with the aid of a ball mill.

Supplementary Information The online version contains supplementary material available at https://doi.org/10.1007/s11664-023-10770-7.

Acknowledgments This research work was financially supported by the Management of CHRIST (Deemed to be University), Bangalore. The authors (A. G. Kunjomana and Bibin John) express their gratitude towards the Centre for Research, CHRIST (Deemed to be University), Bangalore for the research grant extended in order to execute the present project (MRPDSC-1718). Special acknowledgement goes to the Centre for Nano Science and Engineering (CeNSE), Indian Institute of Science (IISc), Bangalore, for the timely assistance in performing FESEM and EDAX characterization of the samples. Heartfelt thanks to the Sophisticated Test and Instrumentation Centre (STIC), Cochin University of Science and Technology (CUSAT), Kerala, and Sophisticated Analytical Instrument Facilities (SAIF), Mahatma Gandhi University, Kerala for their valuable support in availing the opportunity for the characterizations PXRD, UV-Vis-NIR, HRTEM, and PL analysis.

Funding The authors have not disclosed any funding.

Data availability All data generated or analyzed during this study have been deposited in this manuscript. All the compared data were properly cited and included in the reference section following the journal style.

Conflict of interest I hereby confirm that the work described has not been published before, it is not under consideration for publication by any other journal, and publication has been approved by all co-authors and the responsible authorities at the institute(s) where the work was carried out. The authors declare that they have no financial interests.

References

1. X. Guan, P. Lu, L. Wu, L. Han, G. Liu, Y. Song, and S. Wang, Thermoelectric properties of SnSe compound. *J. Alloys Compd.* 643, 116 (2015).
2. C. Zhang, H. Ouyang, R. Miao, Y. Sui, H. Hao, Y. Tang, J. You, X. Zheng, Z. Xu, X.A. Cheng, and T. Jiang, Anisotropic nonlinear optical properties of a SnSe flake and a novel perspective for the application of all-optical switching. *Adv. Opt. Mater.* 7, 1900641 (2019).
3. J.J. Wang, F.F. Cao, L. Jiang, Y.G. Guo, W.P. Hu, and L.J. Wan, High performance photodetectors of individual InSe single crystalline nanowire. *J. Am. Chem. Soc.* 131, 15602 (2009).
4. X. Hun, S. Wang, S. Mei, H. Qin, H. Zhang, and X. Luo, Photoelectrochemical dopamine sensor based on a gold electrode modified with SnSe nanosheets. *Microchim. Acta* 184, 3333 (2017).
5. Z. Nabi, A. Kellou, S. Mecabih, A. Khalfi, and N. Benosman, Opto-electronic properties of rutile SnO_2 and orthorhombic SnS and SnSe compounds. *Mater. Sci. Eng. B* 98, 104 (2003).
6. W.J. Baumgardner, J.J. Choi, Y.F. Lim, and T. Hanrath, SnSe nanocrystals: synthesis, structure, optical properties, and surface chemistry. *J. Am. Chem. Soc.* 132, 9519 (2010).
7. A.G. Kunjomana, J. Bibin, R. Karthikeyan, and S. Varadharajaperumal, Effect of supercooling on the microstructural development and optimization of physical properties of melt grown SnSe crystals. *J. Mater. Sci. Mater. Electron.* 30, 14300 (2019).
8. S. Zhao, H. Wang, Y. Zhou, L. Liao, Y. Jiang, X. Yang, G. Chen, M. Lin, Y. Wang, H. Peng, and Z. Liu, Controlled synthesis of single-crystal SnSe nanoplates. *Nano Res.* 8, 288 (2015).
9. C. Guillen, J. Montero, and J. Herrero, Characteristics of SnSe and $SnSe_2$ thin films grown onto polycrystalline SnO_2-coated glass substrates. *Physica Status Solidi (a)* 208, 679 (2011).
10. J. Liu, Q. Huang, Y. Qian, Z. Huang, F. Lai, L. Lin, M. Guo, W. Zheng, and Y. Qu, Screw dislocation-driven growth of the layered spiral-type SnSe nanoplates. *Cryst. Growth Des.* 16, 2052 (2016).
11. W. Wang, Y. Geng, Y. Qian, C. Wang, and X. Liu, A convenient, low temperature route to nanocrystalline SnSe. *Mater. Res. Bull.* 34, 403 (1999).
12. M. Achimovičová, A. Rečnik, M. Fabián, and P. Baláž, Characterization of tin selenides synthesized by high-energy milling. *Acta. Montanistica. Slovaca.* 16, 123 (2011).
13. E. Dutková, M.J. Sayagués, J. Kováč, J. Kováč Jr., Z. Bujňáková, J. Briančin, A. Zorkovská, P. Baláž, and J. Ficeriová, Mechanochemically synthesized nanocrystalline ternary $CuInSe_2$ chalcogenide semiconductor. *Mater. Lett.* 173, 182 (2016).
14. L.Y. Nee, Z.A. Talib, Z. Zainal, and J.L.Y. Chyi, Synthesis and characterization of copper selenide and tin selenide powders by mechanical alloying method. *Solid State Phenom.* 317, 152 (2021).
15. J. Bibin and A.G. Kunjomana, Facile synthesis of novel antimony selenide nanocrystals with hierarchical architecture by physical vapor deposition technique. *J. Appl. Crystallogr.* 52, 312 (2019).
16. R.A. Varin, T. Czujko, and Z.S. Wronski, *Nanomaterials for solid state hydrogen storage* (Berlin: Springer, 2009).
17. D.S. Kumar, B.J Kumar, H.M. Mahesh, Quantum nanostructures (QDs): an overview, in *Synthesis of Inorganic Nanomaterials*, p. 88, (2018).
18. S.K. Kulkarni, *Nanotechnology: principles and practices* (Berlin: Springer, 2014).
19. J. Gou, J. Zhuge, F. Liang, Processing of polymer nanocomposites, in *Manufacturing Techniques for Polymer Matrix Composites (PMCs)* (Woodhead Publishing, 2012) 119.
20. B.D. Cullity, *Elements of x-ray diffraction* (Boston: Addison-Wesley Publishing, 1956).

21. Y. Leng, *Materials characterization: introduction to microscopic and spectroscopic methods* (New York: Wiley, 2009).
22. P.K. Giri, S. Bhattacharyya, D.K. Singh, R. Kesavamoorthy, B.K. Panigrahi, and K.G.M. Nair, Correlation between microstructure and optical properties of ZnO nanoparticles synthesized by ball milling. *J. Appl. Phys.* 102, 093515 (2007).
23. M.A. Franzman, C.W. Schlenker, M.E. Thompson, and R.L. Brutchey, Solution-phase synthesis of SnSe nanocrystals for use in solar cells. *J. Am. Chem. Soc.* 132, 4060 (2010).
24. H. Jahangiri, S. Sönmez, and M.L. Öveçoğlu, Influence of Milling Media on the mechanical alloyed W-0.5 wt. Ti powder alloy. *Indian J. Mater. Sci.* (2016). https://doi.org/10.1155/2016/7981864.
25. Y.X. Chen, Z.H. Ge, M. Yin, D. Feng, X.Q. Huang, W. Zhao, and J. He, Understanding of the extremely low thermal conductivity in high-performance polycrystalline SnSe through potassium doping. *Adv. Funct. Mater.* 26, 6836 (2016).
26. Z. Li, L. Peng, Y. Fang, Z. Chen, D. Pan, and M. Wu, Synthesis of colloidal SnSe quantum dots by electron beam irradiation. *Radiat. Phys. Chem.* 80, 1333 (2011).
27. P.C. Angelo, *Materials characterization* (Amsterdam: Elsevier, 2014).
28. Z. Wu, Y. Liang, E. Fu, J. Du, P. Wang, Y. Fan, and Y. Zhao, Effect of ball milling parameters on the refinement of tungsten powder. *Metals* 8, 281 (2018).
29. A.M. Smith and S. Nie, Semiconductor nanocrystals: structure, properties, and band gap engineering. *Acc. Chem. Res.* 43, 190 (2010).
30. B.S. Murty, P. Shankar, B. Raj, B.B. Rath, and J. Murday, *Textbook of nanoscience and nanotechnology* (Berlin: Springer, 2013).
31. L. Das, A. Guleria, and S. Adhikari, Aqueous phase one-pot green synthesis of SnSe nanosheets in a protein matrix: negligible cytotoxicity and room temperature emission in the visible region. *RSC Adv.* 5, 61390 (2015).
32. G. Han, S.R. Popuri, H.F. Greer, J.W.G. Bos, W. Zhou, A.R. Knox, A. Montecucco, J. Siviter, E.A. Man, M. Macauley, and D.J. Paul, Facile surfactant-free synthesis of *p*-type SnSe nanoplates with exceptional thermoelectric power factors. *Angew. Chem. Int. Ed.* 55(22), 6433 (2016).